Inorg. Chem. **2007**, *46*, 8728–8738

Infrared and DFT Investigations of the XC≡ReX_3 and HC≡ReX_3 Complexes: Jahn–Teller Distortion and the Methylidyne C–X(H) Stretching Absorptions

Jonathan T. Lyon,[†] Han-Gook Cho,[‡] Lester Andrews,*[,†] Han-Shi Hu,[§] and Jun Li*[,§]

Department of Chemistry, University of Virginia, Charlottesville, Virginia 22904-4319, Department of Chemistry, University of Incheon, 177 Dohwa-dong, Nam-ku, Incheon, 402-749, South Korea, and Department of Chemistry and Key Laboratory of Organic Optoelectronics and Molecular Engineering of Ministry of Education, Tsinghua University, Beijing 100084, China

Received May 24, 2007

The XC≡ReX_3 complexes (X = F, Cl) are produced by CX_4 reaction with laser-ablated Re atoms, following oxidative C–X insertion and α-halogen migration in favor of the carbon–metal triple bond and are identified through the observation of characteristic absorptions in the argon matrix infrared spectra and comparison with vibrational frequencies calculated by density functional theory. The methylidyne C–F and C–Cl stretching absorptions are observed near 1584 and 1328 cm^{-1}, and the C–H stretching modes for HC≡ReX_3 at 3104 and 3097 cm^{-1}, respectively, which are substantially higher than the precursor stretching modes and in agreement with the general trend that higher s-orbital character in carbon hybridization leads to a higher stretching frequency. The Jahn–Teller effect in the doublet-state XC≡ReX_3 and HC≡ReX_3 complexes gives rise to distorted structures with C_s symmetry and two equivalent longer Re–X bonds and one slightly shorter Re–X bond.

Introduction

Transition metal complexes with carbon−metal triple bonds have been extensively studied due to their versatile chemistry, reactivities, and catalytic activities,[1,2] but only a few of them contain the simple M≡C−H moiety and even fewer involve the halogen substituent as M≡C−X (M = transition metal, particularly rhenium).[1−5] Although the C−H vibrational characteristics are difficult to investigate due to very low infrared intensity and interference from other hydrogen stretching absorptions, the C−X stretching bands are very intense and fall in a clean region of the spectrum and can be used as a probe to study the orbital hybridization and bonding at carbon. Recently we prepared the doublet ground state HC≡ReH_3 complex in solid argon for observation of the C−H stretching mode at 3101.8 cm^{-1}, and density functional calculations reveal 45.6% s character in the C hybrid orbital and a distorted geometry of C_s symmetry.[6] This fundamentally important simple methylidyne complex can be investigated by high level theoretical calculations to understand the unique bonding and structure around the Re center including Jahn−Teller distortion and symmetry reduction. The present work was designed in part to determine the effect of halide substituents on the C≡Re bond and their effect on the symmetry at the rhenium center with the possibility of Jahn−Teller distortion and the hybridization at carbon.

Recent work in this laboratory lead to the discovery of a new class of electron-deficient triplet-state methylidyne complexes XC÷MX_3 from a Group 4 atom reacting with CX_4 (X = F, Cl) molecules. Chlorofluoromethanes were also investigated, and both possible structural isomers were observed. The thermochemical driving force for complete α-F transfer dominated these reactions and provided a very high diagnostic C−F stretching mode in the 1453−1413

* To whom correspondence should be addressed. E-mail: lsa@virginia.edu (L.A.); junli@tsinghua.edu.cn (J.L.).
† University of Virginia.
‡ University of Incheon.
§ Tsinghua University.

(1) (a) Schrock, R. R. *Chem. Rev.* **2002**, *102*, 145 (review article). (b) Herndon, J. W. *Coord. Chem. Rev.* **2004**, *248*, 3.
(2) Da Re, R. E.; Hopkins, M. D. *Coord. Chem. Rev.* **2005**, *249*, 1396.
(3) Nugent, W. A.; Mayer, J. M. *Metal-Ligand Multiple Bonds*; John Wiley and Sons: New York, 1988.
(4) Almedia, S. S. P. R.; Pomberio, A. J. L. *Organometallics* **1997**, *16*, 4469.
(5) Carvalho, M. F. N. N.; Almedia, S. S. P. R.; Pomberio, A. J. L. *Organometallics* **1997**, *16*, 5441.
(6) Cho, H.-G.; Andrews, L. *Organometallics* **2007**, *26*, 4098 (HC≡ReH_3 complex).

10.1021/ic701014u CCC: $37.00
Published on Web 09/19/2007

cm^{-1} region.[7−9] Fluoro and chloro carbyne complexes of rhenium have been synthesized from protonation of vinylidene precursors, and the formation of the carbyne complexes demonstrated the stability of the rhenium−carbon triple bond.[4,5] Accordingly, we have designed reactions of laser-ablated Re atoms with CX_4 and CHX_3 precursors (X = F, Cl) to look for new carbyne complexes of rhenium formed by complete α-halogen transfer.

Experimental and Computational Methods

Laser-ablated Re atoms (Johnson−Matthey) were reacted with CF_4, CF_3Cl (DuPont), CF_3Br (Peninsular), $^{13}CF_3Cl$, $^{13}CF_3Br$ (prepared),[10,11] CCl_4, and $^{13}CCl_4$ (MSD Isotopes) in excess argon during condensation at 8 K using a closed-cycle refrigerator (Air Products HC-2). These methods have been described in detail elsewhere.[12,13] Reagent gas mixtures were typically 0.5−1% in argon. After reactions, infrared spectra were recorded at a resolution of 0.5 cm^{-1} using a Nicolet 550 spectrometer with an MCT-B detector. Samples were later irradiated for 20 min periods by a mercury arc lamp (175 W) with the globe removed using a combination of optical filters, and then samples were annealed to allow reagent diffusion.

Density functional theory (DFT) calculations were carried out using the Gaussian 03 package,[14] the hybrid B3LYP density functional,[15] the 6-311++G(3df,3pd) basis sets for C, H, F, Cl, and Br,[16] and SDD pseudopotential and basis set[17] for Re to provide a consistent set of vibrational frequencies for the reaction products. Geometries were fully relaxed during optimizations, and the stationary nature of the optimized geometries was confirmed by vibrational analysis. All of the vibrational frequencies were calculated analytically. Zero-point energies were included in the calculation of reaction energies. Natural bond orbitals, natural localized molecular orbitals, natural population analysis, and natural Wiberg bond orders were calculated to help understand the bonding and electronic structures of the molecules under consideration.[18] To further validate the calculated B3LYP geometries and vibrational frequencies, electronic structure calculations were also performed using quasi-relativistic DFT with the generalized gradient PW91 approach implemented in Amsterdam Density Functional program (ADF 2006.01).[19] In the PW91 calculations, the zero-order-regular approximation (ZORA) was used to account for the scalar and spin−orbit coupling relativistic effects[20] and uncontracted Slater basis sets with triple-ζ plus two polarization functions (TZ2P)[21] were employed. The frozen core approximation was applied to the [1s^2] cores of C and F, [1s^2 2p^6] core of Cl, and [1s^2 4f^{14}] core of Re, with the rest of the electrons explicitly treated variationally.[22] The geometries were fully optimized with inclusion of the scalar relativistic effects and tight convergence criteria for the energy gradients were utilized. Vibrational frequency calculations were accomplished by numerical differentiation of the energy gradients. Diabatic bond energies are calculated with zero point energy corrections. We also performed fragment molecular orbital calculations using the PW91 functional and linear synchronous transit (LST) calculations to analyze the orbital interactions and the Jahn−Teller effects.

Results and Discussion

The products of rhenium atoms reacting with CF_4, CF_3Cl, CF_3Br, CCl_4, and haloforms will be characterized by matrix infrared spectra and DFT calculations. Jahn−Teller distortion and bonding trends in doublet-state methylidyne product complexes will be discussed. These experiments also reveal absorptions due to precursor fragment and parent anion reactive species that have been reported previously,[10,11,23] as well as new C−H stretching bands for the parent anion.

Re + CF_4. The reactions of laser-ablated rhenium atoms and carbon tetrafluoride produced new infrared absorptions at 1585.3, 662.9, 654.6, and 607.8 cm^{-1}, which are illustrated in Figures 1 and 2 (the product bands are marked with arrows) and listed in Table 1. These bands were not affected by ultraviolet (UV) irradiation, but they sharpened slightly on annealing to 30 K.

Re + CF_3Cl. Reactions between laser-ablated Re atoms and CF_3Cl (Freon-13) yield similar absorptions at 1583.3, 643.4, and 610.0 cm^{-1}. While these absorptions did not change with 300−380 nm irradiation, they increased by 20% with >290 nm light and another 50% with >220 nm irradiation but decreased 10% on annealing to 30 K. The

(7) Lyon, J. T.; Andrews, L. *Inorg. Chem.* **2006**, *45*, 9858 (Ti + CF_4).
(8) Lyon, J. T.; Andrews, L. *Organometallics* **2007**, *26*, 2519 (Gr 4 + CF_2Cl_2).
(9) Lyon, J. T.; Andrews, L. *Organometallics* **2007**, *26*, 4152 (Gr 4 + CF_3X) .
(10) Prochaska, F. T.; Andrews, L. *J. Chem. Phys.* **1978**, *68*, 5577.
(11) (a) Prochaska, F. T.; Andrews, L. *J. Am. Chem. Soc.* **1978**, *100*, 2102. (b) Andrews, L.; Willner, H.; Prochaska, F. T. *J. Fluorine Chem.* **1979**, *13*, 273.
(12) Andrews, L.; Citra, A. *Chem. Rev.* **2002**, *102*, 885 and references therein.
(13) Andrews, L. *Chem. Soc. Rev.* **2004**, *33*, 123 and references therein.
(14) Frisch, M. J.; Trucks, G. W.; Schlegel, H. B.; Scuseria, G. E.; Robb, M. A.; Cheeseman, J. R.; Montgomery, J. A., Jr.; Vreven, T.; Kudin, K. N.; Burant, J. C.; Millam, J. M.; Iyengar, S. S.; Tomasi, J.; Barone, V.; Mennucci, B.; Cossi, M.; Scalmani, G.; Rega, N.; Petersson, G. A.; Nakatsuji, H.; Hada, M.; Ehara, M.; Toyota, K.; Fukuda, R.; Hasegawa, J.; Ishida, M.; Nakajima, T.; Honda, Y.; Kitao, O.; Nakai, H.; Klene, M.; Li, X.; Knox, J. E.; Hratchian, H. P.; Cross, J. B.; Bakken, V.; Adamo, C.; Jaramillo, J.; Gomperts, R.; Stratmann, R. E.; Yazyev, O.; Austin, A. J.; Cammi, R.; Pomelli, C.; Ochterski, J. W.; Ayala, P. Y.; Morokuma, K.; Voth, G. A.; Salvador, P.; Dannenberg, J. J.; Zakrzewski, V. G.; Dapprich, S.; Daniels, A. D.; Strain, M. C.; Farkas, O.; Malick, D. K.; Rabuck, A. D.; Raghavachari, K.; Foresman, J. B.; Ortiz, J. V.; Cui, Q.; Baboul, A. G.; Clifford, S.; Cioslowski, J.; Stefanov, B. B.; Liu, G.; Liashenko, A.; Piskorz, P.; Komaromi, I.; Martin, R. L.; Fox, D. J.; Keith, T.; Al-Laham, M. A.; Peng, C. Y.; Nanayakkara, A.; Challacombe, M.; Gill, P. M. W.; Johnson, B.; Chen, W.; Wong, M. W.; Gonzalez, C.; Pople, J. A. *Gaussian 03*, revision B.04; Gaussian, Inc.: Wallingford, CT, 2004.
(15) (a) Becke, A. D. *J. Chem. Phys.* **1993**, *98*, 5648. (b) Lee, C.; Yang, Y.; Parr, R. G. *Phys. Rev. B* **1988**, *37*, 785.
(16) Frisch, M. J.; Pople, J. A.; Binkley, J. S. *J. Chem. Phys.* **1984**, *80*, 3265.
(17) Andrae, D.; Haeussermann, U.; Dolg, M.; Stoll, H.; Preuss, H. *Theor. Chim. Acta* **1990**, *77*, 123.
(18) (a) Reed, A. E.; Weinstock, R. B.; Weinhold, F. *J. Chem. Phys.* **1985**, *83*, 735. (b) Reed, A. E.; Curtiss, L. A.; Weinhold, F. *Chem. Rev.* **1988**, *88*, 899. (c) Wiberg, K. B. *Tetrahedron* **1968**, *24*, 1083.
(19) ADF 2006.01, SCM, Theoretical Chemistry, Vrije Universiteit, Amsterdam, The Netherlands (http://www.scm.com). (a) te Velde, G.; Bickelhaupt, F. M.; van Gisbergen, S. J. A.; Fonseca Guerra, C.; Baerends, E. J.; Snijders, J. G.; Ziegler, T. *J. Comput. Chem.* **2001**, *22*, 931. (b) Fonseca Guerra, C.; Snijders, J. G.; te Velde, G.; Baerends, E. J. *Theor. Chem. Acc.* **1998**, *99*, 391. (c) Perdew, J. P.; Wang, Y. *Phys. Rev. B* **1992**, *45*, 13244.
(20) van Lenthe, E.; Baerends, E. J.; Snijders, J. G. *J. Chem. Phys.* **1993**, *99*, 4597.
(21) van Lenthe, E.; Baerends, E. J. *J. Comp. Chem.* **2003**, *24*, 1142.
(22) Baerends, E. J.; Ellis, D. E.; Ros, P. *Chem. Phys.* **1973**, *2*, 42.
(23) (a) Milligan, D. E.; Jacox, M. E.; McAuley, J. H.; Smith, C. E. *J. Mol. Spectrosc.* **1973**, *45*, 377. (b) Prochaska, F. T.; Andrews, L. *J. Phys. Chem.* **1978**, *82*, 1731. (c) Andrews, L.; Prochaska, F. T. *J. Phys. Chem.* **1979**, *83*, 824. (d) Andrews, L.; Prochaska, F. T. *J. Am. Chem. Soc.* **1979**, *101*, 1190. (Cl^-)($HCCl_2$).

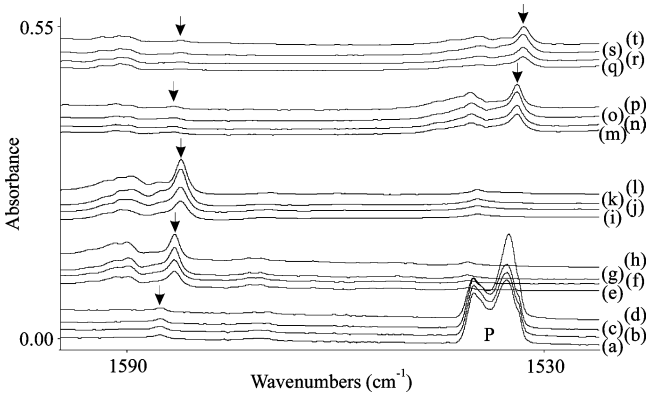

Figure 1. Infrared spectra in the 1500 cm^{-1} region for the Re atom reaction product with CX_4 molecules in excess argon at 8 K. (a) Re + 1.0% CF_4 in argon co-deposited for 1 h. (b) After irradiation (λ < 290 nm). (c) After irradiation (λ > 220 nm). (d) After annealing to 30 K. (e) Re + 1.0% CF_3-Cl in argon co-deposited for 1 h. (f) After irradiation (< 290 nm). (g) After irradiation (λ > 220 nm). (h) After annealing to 30 K. (i) Re + 1.0% CF_3Br in argon, (j) After irradiation (λ < 290 nm). (k) After irradiation (λ > 220 nm). (l) After annealing to 30 K, (m) Re + 1.0% $^{13}CF_3Cl$ in argon, (n) After irradiation (λ < 290 nm). (o) After irradiation (λ > 220 nm). (p) After annealing to 30 K, (q) Re + 1.0% $^{13}CF_3Br$ in argon, (r) After irradiation (λ < 290 nm). (s) After irradiation (λ > 220 nm). (t) After annealing to 30 K. Arrows denote the methylidyne complex absorption, and P denotes precursor bands.

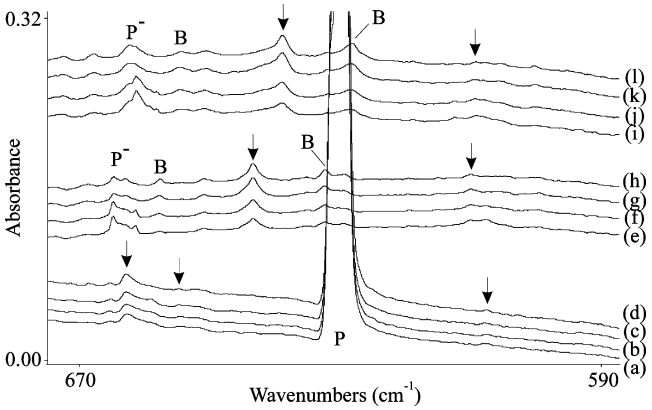

Figure 2. Infrared spectra in the 600 cm^{-1} region for the Re atom reaction product in the first three sets of four spectra in Figure 1. P denotes precursor and P^- marks parent anion absorption.

spectra are compared in Figures 1 and 2. Other bands at 657.8 and 632.4 cm^{-1} (marked B) increased on the initial photolysis and more with the last irradiation for a total 4-fold growth. The sharp 664.9 cm^{-1} band has a ^{13}C counterpart at 655.8 cm^{-1}, which have been identified as the parent anion in earlier studies. These photosensitive bands are common to other metal experiments.[9,10] The ^{13}C sample produced analogous bands at 1534.0 (Figure 1), 643.2 and 610.0 cm^{-1}. The B bands were found at 657.8 and 632.2 cm^{-1}. The new absorptions are collected in Table 2.

Re + CF_3Br. Likewise, the reactions with CF_3Br formed similar products with slightly shifted absorptions at 1582.4, 638.9, and 609.4 cm^{-1}, which increased similarly on UV irradiation, and another pair (marked B) at 654.6 and 628.2 cm^{-1}. The photosensitive parent anion is now at 661.4 and 651.9 cm^{-1} with the two carbon isotopes. In the first set of bands, only the upper band shifted using $^{13}CF_3Br$, namely to 1533.1 cm^{-1} (Figure 1 and Table 3). The 654.6 cm^{-1} band was not shifted, but the 628.2 cm^{-1} counterpart was displaced to 628.0 cm^{-1}.

Re + CCl_4. Experiments with carbon tetrachloride gave a strong doublet at 1328.0, 1322.5 cm^{-1}, which shifted to 1280.0, 1275.2 cm^{-1} with ^{13}C-enriched material as shown in Figure 3. These bands increased about 10% on >290 nm radiations, 20% on >220 nm irradiations, and another 20% on annealing to 30 K.

Re + CHX_3. Rhenium reactions with fluoroform gave rise to new absorptions at 3103.8, 688.8, 657.1, 652.0, 614.1, 602.8, and 628.8 cm^{-1}, which are compared in Figure 4 with the spectra from analogous chloroform reactions. UV irradiation tripled the first six new fluoroform product absorptions after their formation on co-deposition of laser-ablated Re and reagent molecules in excess argon but failed to change the last one. Annealing had no effect on these absorptions. On the other hand, the chloroform product bands increased 20−30% on the UV irradiations and about 40% on annealing to 30 K. In the chloroform case, the upper band falls at 3097.3 cm^{-1}, shifts to 3086.1 cm^{-1} with ^{13}C, and shifts to 2329.4 cm^{-1} on deuterium substitution. The weak 3087.2 cm^{-1} band destroyed by >290 nm irradiation shifts to 3076.6 cm^{-1} with ^{13}C and to 2304.6 cm^{-1} on deuterium substitution: these new bands are common to other metal experiments, and are, we believe, due to the parent anion. In the lower region, new absorptions are observed at 669 (shoulder) and 623.9 cm^{-1} for chloroform, 663.5 and 618.9 cm^{-1} for $^{13}CHCl_3$, and at 534.4 and 494.8 cm^{-1} for $CDCl_3$ reactions.

In order to determine if the sharp, new highest frequency absorption could be tuned by replacing fluorine with chlorine, the mixed fluorochloroforms were employed. The CHF_2Cl precursor reacted with Re to give new bands at 3101.6, 688.6, 644.5, 638.6, 620.7, and 615.8 cm^{-1}, which are shown in Figure 4. With $^{13}CHF_2Cl$, these bands shifted to 3090.6, 685.5, 643.6, 638.2, 620.3, and 615.6 cm^{-1}. Rhenium and $CHFCl_2$ gave product absorptions at 3099.5, 682.1, 638.5, and 597.7 cm^{-1}, which shifted to 2331.1, 538.7, 634.8, and 476.7 cm^{-1} with the $CDFCl_2$ reagent. Photosensitive parent anion counterparts were found at 3081.6, 656.0 and at 2301.0, 550.5 cm^{-1}.

Product Identification. XC≡ReX_3. On the basis of our previous work with methane activation by transition metal atoms,[24] three reaction products are possible. The Grignard-type insertion product (CF_3−ReF) in the sextet state is predicted by B3LYP density functional calculations to be 34 kcal/mol lower than the sum of the energies of the reactants Re and CF_4. This molecule has a Re−F stretching mode at 595 cm^{-1} (201 km/mol intensity), which is 63 cm^{-1} lower than the strongest Re−F stretching mode calculated for the product assigned here (Table 1). The highest frequency C−F stretching mode calculated for this insertion product is 1146 cm^{-1}, which is substantially below the observed 1585 cm^{-1} band. The quartet-state methylidene product (CF_2=ReF_2) is predicted to also be 64 kcal/mol lower

(24) Andrews, L.; Cho, H.-G. *Organometallics* **2006**, *25*, 4040 and references therein (review article).

Table 1. Observed and Calculated Fundamental Frequencies of FC≡ReF_3 and ClC≡$ReCl_3$ in the Ground $^2A'$ Electronic State with C_s Structure[a]

approximate description	FC≡ReF_3 obs	FC≡ReF_3 calcd	FC≡ReF_3 int	F^{13}C≡ReF_3 calcd	F^{13}C≡ReF_3 int	ClC≡$ReCl_3$ obs	ClC≡$ReCl_3$ calcd	ClC≡$ReCl_3$ int	Cl^{13}C≡$ReCl_3$ obs	Cl^{13}C≡$ReCl_3$ calcd	Cl^{13}C≡$ReCl_3$ int
C−F/C−Cl stretch,[b] a′	1585.3	1622.2	382	1570.7	362	1328.0	1346.9	171	1280.2	1297.9	160
ReF_2/$ReCl_2$ stretch, a′	662.9	658.3	145	658.3	145		387.9	87		386.7	88
Re−F/Re−Cl stretch, a′	654.6	645.1	88	644.9	88		377.0	7		375.4	9
XC≡Re stretch, a′	−[c]	623.5	12	619.6	11		343.9	7		334.3	4
ReF_2/$ReCl_2$ stretch, a″	607.8	603.6	84	603.6	84		369.2	31		368.7	36
XCRe bend, a′		422.1	3	408.2	2		438.1	15		437.3	14
XCRe bend, a″		392.5	10	379.8	9		346.9	25		334.8	19

[a] Frequencies and intensities are in cm^{-1} and km/mol, respectively. Five lower real frequencies are not listed. Observed natural isotopic frequencies in an argon matrix. Frequencies and intensities were calculated with B3LYP/6-311++G(3df,3pd), and the SDD pseudopotential and basis set are used for Re. The symmetry notations are based on the C_s structure. [b] Mixed mode with some C≡Re stretching character. [c] Possibly masked by CF_4 precursor.

Table 2. Observed and Calculated Fundamental Frequencies of FC≡ReF_2Cl and ClC≡ReF_3 in Ground $^2A'$ Electronic States with C_s Structures[a]

approximate description	FC≡ReF_2Cl obs	FC≡ReF_2Cl calcd	FC≡ReF_2Cl int	F^{13}C≡ReF_2Cl obs	F^{13}C≡ReF_2Cl calcd	F^{13}C≡ReF_2Cl int	ClC≡ReF_3 obs	ClC≡ReF_3 calcd	ClC≡ReF_3 int	Cl^{13}C≡ReF_3 obs	Cl^{13}C≡ReF_3 calcd	Cl^{13}C≡ReF_3 int
C−F/C−Cl stretch,[b] a′	1583.3	1627.0	448	1534.0	1575.4	−[c]		1350.4	112	−[c]	1301.2	104
ReF_2 stretch, a′	643.4	651.1	132	643.3	651.1		657.8	658.3	149	657.8	658.2	148
Re−F stretch, a′		622.5	16	618.9		16	632.4	641.2	101	632.2	641.0	102
C≡Re stretch, a′	610.0	606.2	79	610.0	606.2	79		605.7	82		605.7	83
ReF_2 stretch, a″		436.0	11	383.6		34		447.6	15		445.1	14
FCRe bend, a′		395.0	7	423.0		15		375.9	2		364.9	3
Re−Cl stretch		385.1	38	382.0		7		328.8	15		317.3	14

[a] Frequencies and intensities are in cm^{-1} and km/mol, respectively. Five lower real frequencies are not listed. Observed natural isotopic frequencies in an argon matrix. Frequencies and intensities were calculated with B3LYP/6-311++G(3df,3pd), and the SDD pseudopotential and basis set are used for Re. The symmetry notations are based on the C_s structure. [b] Mixed mode with some C≡Re stretching character. [c] Possibly masked by CF_3Cl precursor.

Table 3. Observed and Calculated Fundamental Frequencies of FC≡ReF_2Br and BrC≡ReF_3 Complexes in the Ground $^2A'$ Electronic States with C_s Structures[a]

approximate description	FC≡ReF_2Br obs	FC≡ReF_2Br calcd	FC≡ReF_2Br int	F^{13}C≡ReF_2Br obs	F^{13}C≡ReF_2Br calcd	F^{13}C≡ReF_2Br int	BrC≡ReF_3 obs	BrC≡ReF_3 calcd	BrC≡ReF_3 int	Br^{13}C≡ReF_3 obs	Br^{13}C≡ReF_3 calcd	Br^{13}C≡ReF_3 int
C−F/C−Br stretch,[b] a′	1582.4	1624.0	472	1533.1	1572.5	447	−[c]	1281.0	63	−[c]	1233.0	57
ReF_2 stretch, a′	638.9	649.1	141	638.9	649.1	141	654.6	658.4	150	654.6	658.4	149
Re−F stretch,a′		621.4	16		617.8	16	628.2	640.8	109	628.0	640.6	109
C≡Re stretch, a′	609.4	606.2	77	609.4	606.2	77		606.2	82		606.2	82
ReF_2 stretch, a″		433.7	4		419.2	4		375.5	9		363.7	9
FCRe bend, a′		393.5	7		380.6	6		302.9	5		302.2	5
Re−Cl stretch		266.8	2		266.5	22		301.4	16		290.7	15

[a] Frequencies and intensities are in cm^{-1} and km/mol, respectively. Five lower real frequencies are not listed. Observed natural isotopic frequencies in an argon matrix. Frequencies and intensities were calculated with B3LYP/6-311++G(3df,3pd), and the SDD pseudopotential and basis set are used for Re. The symmetry notations are based on the C_s structure. [b] Mixed mode with some C≡Re stretching character. [c] Possibly masked by CF_3Cl precursor.

in energy than the reagents combined. It has strong C−F stretching absorptions at 1280 and 1160 cm^{-1}, which are also much too low to fit the observed band. However, the third possibility, namely the methylidyne (FC≡ReF_3) in the doublet ground state, is calculated to be the most stable among the plausible products, namely 50 kcal/mol more stable than the insertion and 20 kcal/mol more stable than the methylidene complex and 84 kcal/mol *lower* in energy than Re + CF_4. More importantly, the strongest absorption is predicted at 1622.2 cm^{-1}, which is in very good agreement with the observed 1585.3 cm^{-1} frequency for the density functional calculation. Furthermore, the calculation gives a ^{13}C shift of 51.5 cm^{-1} for this C−F stretching mode, which is in line with what we observe for the Freon-13 counterpart absorption at 1583.3 cm^{-1}. The calculated frequency is 36.9 cm^{-1} or 2.3% higher than the observed value, which is usual for the B3LYP approach and is within the error bar of the DFT calculations with harmonic approximation involved.[15−17]

The single C−F bond stretching mode discussed above is calculated to be the strongest IR absorption for FC≡ReF_3, and we can expect the relative intensities calculated by DFT to provide an approximate guide for other modes. Figure 2 also illustrates three other associated product absorptions at 662.9, 654.6, and 607.8 cm^{-1}. The 662.9 cm^{-1} band is slightly stronger than the 1585.3 cm^{-1} band, but the last two bands are weaker. All three are in the region expected for Re−F stretching modes, between values for solid ReF_4 and ReF_5 (660−722 cm^{-1} range) and for ReF (565 cm^{-1}).[25,26] These Re−F stretching absorptions are consistent with the

(25) Paine, R. T.; Asprey, L. B. *Inorg. Chem.* **1975**, *14*, 1111 (ReF_4, ReF_5).
(26) Launila, O.; James, A. M.; Simard, B. *J. Mol. Spectrosc.* **1994**, *164*, 559 (ReF).

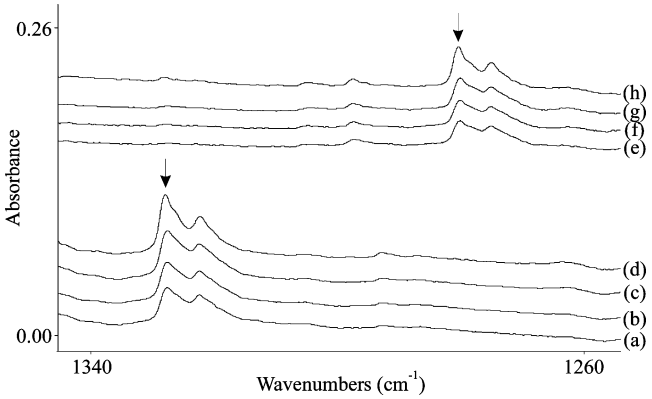

Figure 3. Infrared spectra in the 1350−1250 cm^{-1} region for the product of Re atom reaction with CCl_4 and $^{13}CCl_4$ in excess argon. (a) Re + 1.0% CCl_4 in argon co-deposited for 1 h. (b) After photolysis (λ < 290 nm). (c) After photolysis (λ > 220 nm). (d) After annealing to 30 K. (e) Re + 1.0% $^{13}CCl_4$ in argon co-deposited for 1 h. (f) After photolysis (λ < 290 nm). (g) After photolysis (λ > 220 nm). (h) After annealing to 30 K. Arrows denote the product absorptions.

predicted symmetric and antisymmetric Re−F stretching frequencies for the ReF_2 subunit with equivalent Re−F bonds and the single slightly shorter Re−F bond in FC≡ReF_3 as shown in Table 1 (frequencies predicted to be 4.6, 9.5, and 4.2 cm^{-1} lower than observed). We note that the hybrid density functional approach provides good approximate calculations of frequencies, and comparison with results using the pure PW91 density functional (Table S1) substantiates these assignments.[27]

The observation of three different Re−F stretching modes for a molecule with a ReF_3 fragment implies that the symmetry is lower than 3-fold. In fact, the two bond stretching modes (e and a_1) of the trigonal heavy metal methylidyne trifluoride FC≡WF_3 are calculated to be separated by less than 10 cm^{-1}. An additional weak absorption calculated at 623.5 cm^{-1} has considerable C≡Re stretching character, as does the 1662.2 cm^{-1} frequency, but the strong CF_4 band at 630 cm^{-1} precludes any possibility of its detection. Our calculation reveals strong coupling between the C−F and C≡Re stretching modes, and there is substantial separation between the two calculated frequencies involving carbon motion, (1622.2 and 623.5 cm^{-1}). Our observation of four absorptions, which correlate well with the B3LYP and PW91 predictions for the FC≡ReF_3 perfluoro methylidyne complex, substantiates the identification of this species.

Both B3LYP and PW91 frequency calculations (Tables 1 and S1) show that only one absorption can be observed for the perchloro counterpart ClC≡$ReCl_3$ complex, namely the strong C−Cl stretching mode, because the Re−Cl stretching absorptions fall below our 420 cm^{-1} limit of detection. The strong C−Cl stretching mode is predicted at 1346.9 cm^{-1} with a 49.0 cm^{-1} ^{13}C shift by B3LYP and at 1321.4 cm^{-1} with a 48.2 cm^{-1} ^{13}C shift by PW91, and this mode is observed at 1328.0 cm^{-1} with a 47.8 cm^{-1} ^{13}C shift. Notice that the two density functional calculations bracket the

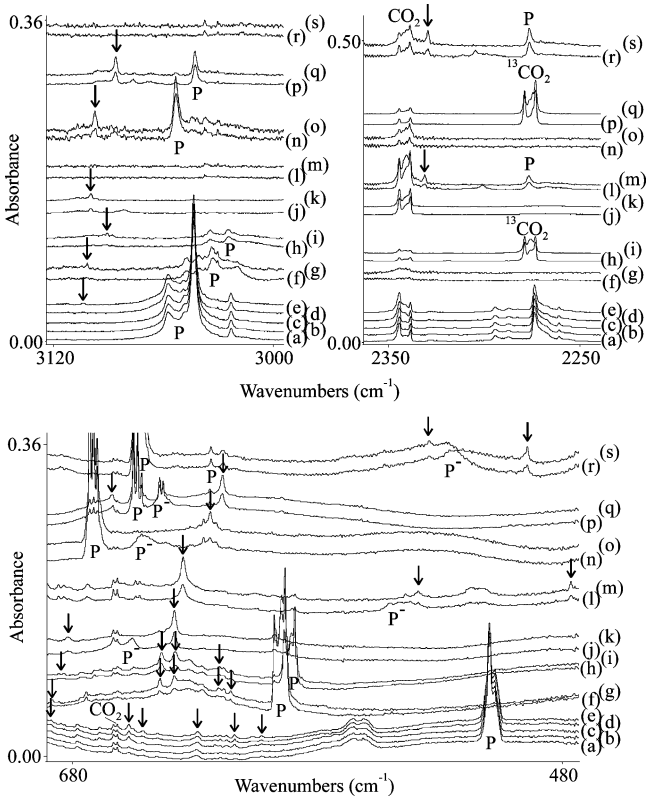

Figure 4. Infrared spectra in the C−H and C−D stretching and bending regions for the Re atom reaction product with CHX_3 molecules in excess argon at 8 K. (a) Re + 1.0% CHF_3 in argon co-deposited for 1 h. (b) After irradiation (λ < 290 nm). (c) After irradiation (λ > 220 nm). (d) After annealing to 30 K. (e) After second λ > 220 nm irradiation. (f) Re + 1.0% CHF_2Cl in argon co-deposited for 1 h. (g) After irradiation (λ < 290 nm), (λ > 220 nm), annealing to 30 K, and second λ > 220 nm irradiation. (h) Re + 1.0% $^{13}CHF_2Cl$ in argon. (i) After combined irradiation and annealing treatment described above. (j) Re + 1.0% $CHFCl_2$ in argon. (k) After combined treatement. (l) Re + 1.0% $CDFCl_2$ in argon. (m) After combined treatment. (n) Re + 1.0% $CHCl_3$ in argon. (o) After combined treatment. (p) Re + 1.0% $^{13}CHCl_3$ in argon. (q) After combined treatment. (r) Re + 1.0% $CDCl_3$ in argon. (s) After combined irradiation cycle. Arrows denote the methylidyne complex absorptions, P denotes precursor bands, and P^- parent anion absorptions.

experimental value. A harmonic C−Cl vibration would shift only 38.7 cm^{-1}, so there is considerable C−Cl and C−Re coupling in this vibration to give an antisymmetric Cl−C−Re motion.

The CF_4 reaction proceeds through the first and second intermediate species via C−F bond activation by excited Re atoms and two successive α-F transfers to form the most stable methylidyne product as outlined by reaction 1, which is overall exothermic by 84 kcal/mol at the B3LYP level of theory. Note that each step is exothermic and that this excess energy activates the next step. The analogous reaction with CCl_4 to form ClC≡$ReCl_3$ is exothermic by 146 kcal/mol, owing to the much weaker C−Cl bond. The ClC≡$ReCl_3$ complex increases by 20% on annealing the sample to 30 K, which suggests that the ground-state Re atom activation of CCl_4 is spontaneous. Very early work showed that Li atoms react spontaneously with CCl_4, but only one Cl is abstracted to form LiCl and the CCl_3 radical.[28] Because the

(27) (a) Scott, A. P.; Radom, L. *J. Phys. Chem.* **1996**, *100*, 16502. (b) Andersson, M. P.; Uvdal, P. L. *J. Phys. Chem. A* **2005**, *109*, 3937.

(28) Andrews, L. *J. Chem. Phys*. **1968**, *48*, 972.

Re−X bonds are much stronger than the C−X bonds, reactions with three halogen atoms transferred to Re are very favorable from a thermochemical standpoint.

$$Re^* + CF_4 \rightarrow [CF_3{-}ReF]^* \rightarrow [CF_2{=}ReF_2]^* \rightarrow FC{\equiv}ReF_3 \quad (1)$$

$$Re + CCl_4 \rightarrow [CCl_3{-}ReCl]^* \rightarrow [CCl_2{=}ReCl_2]^* \rightarrow ClC{\equiv}ReCl_3 \quad (2)$$

The CF_3X (X = Cl, Br) reactions were investigated in order to introduce ^{13}C into the product and to examine the relative yields of the two structural isomers $ClC{\equiv}ReF_3$ and $FC{\equiv}ReF_2Cl$ and their bromine analogues. The spectra in Figure 1 establish conclusively that reaction occurs to form a new product complex with an unusually high C−F stretching mode with more ^{13}C shift than expected for a pure harmonic C−F oscillator.

The diagnostic absorption at 1585.3 cm^{-1} with CF_4 shifts to 1583.3 cm^{-1} with CF_3Cl and to 1582.4 cm^{-1} with CF_3Br. The 90% ^{13}C precursors reveal strong new bands at 1534.0 and 1533.1 cm^{-1}, respectively, and weak bands for the residual ^{12}C, which confirm that this vibrational mode involves a single carbon atom and that the molecule likely contains only one carbon. Both of these carbon isotopic shifts are 49.3 cm^{-1}, which exceeds the 37.9 cm^{-1} value calculated for a simple C−F harmonic oscillator. This result indicates that the C−F stretching mode couples with the C−Re stretching mode. In other words, this mode is in effect an antisymmetric F−C−Re stretching mode, which arises here due to the motion of C between the heavier F and Re atoms. Then we are left with the symmetric counterpart as a FC−Re stretching mode, which is calculated at 436.0 cm^{-1} with a ^{13}C shift of 13.0 cm^{-1} for $FC{\equiv}ReF_2Cl$ and at 433.7 cm^{-1} with a ^{13}C shift of 14.5 cm^{-1} for $FC{\equiv}ReF_2Br$.

Two bands at 643.4 and 610.0 cm^{-1} (marked with arrows) are associated with the 1583.3 cm^{-1} band as they double in intensity during the irradiations. The next strongest band calculated at 651.1 cm^{-1} (Table 2) is the a′ ReF_2 stretching mode, and the observed absorption at 643.4 cm^{-1} is in satisfactory agreement for $FC{\equiv}ReF_2Cl$. The third most intense absorption is predicted to be the a″ ReF_2 stretching mode at 606.2 cm^{-1}, and the 610.0 cm^{-1} band is appropriate for $FC{\equiv}ReF_2Cl$. Analogous bands at 638.9 and 609.4 cm^{-1} (Table 3) are associated with the 1582.4 cm^{-1} band, and all are assigned to the $FC{\equiv}ReF_2Br$ methylidyne complex.

Two additional bands at 657.8 and 632.4 cm^{-1} (marked B following the nomenclature employed for the analogous Group 4 reaction products) increase 4-fold in intensity during the irradiation cycles, and these are in good agreement with two strong bands predicted at 658.3 and 641.2 cm^{-1} for the structural isomer $ClC{\equiv}ReF_3$ complex (Table 2). Note that the C−Cl stretching mode for this complex is predicted to be much weaker than the above C−F stretching mode, and the former is probably masked by other bands in the 1300 cm^{-1} region. Likewise, two additional bands at 654.6 and 628.2 cm^{-1} (marked B) increase together on UV irradiation and are in good agreement with the two strong bands calculated at 658.4 and 640.8 cm^{-1} for the isomer $BrC{\equiv}ReF_3$ complex (Table 3). The C−Br stretching mode is calculated to be weaker still and likely is covered by other absorptions in this region of the spectrum.

On the basis of the relative intensities of the ReF_2 stretching modes at 643.4 and 657.8 cm^{-1} for these two complexes, respectively, the $FC{\equiv}ReF_2Cl$ complex is produced on laser ablation 10-fold more than the isomeric $ClC{\equiv}ReF_3$ complex, but UV irradiation produces twice as much growth in the latter than in the former complex. Our calculations show that these two isomers are nearly degenerate, with the $FC{\equiv}ReF_2Cl$ complex being only 0.7 kcal/mol higher in energy than the $ClC{\equiv}ReF_3$ complex. This energy difference is within the error bar of the DFT calculations. The greater yield of the $FC{\equiv}ReF_2Cl$ complex on the initial reaction is probably due to the faster rate of activation of the weaker C−Cl bond by excited Re atoms and the formation of more initial $CF_3{-}Re{-}Cl$ than $CF_2Cl{-}Re{-}F$ insertion complex in the first reaction step. This insertion and the following two successive α-F transfers gives more $FC{\equiv}ReF_2Cl$ than $ClC{\equiv}ReF_3$; however, UV irradiation in the cold solid matrix tends to favor the lower energy product and the latter complex is enhanced. The same conclusion can be reached for the $FC{\equiv}ReF_2Br$ and $BrC{\equiv}ReF_3$ complexes, but in this case, the former is more stable than the latter by 1.7 kcal/mol. A similar preference for the analogous Group 4 electron-deficient methylidyne complexes has been found previously.[8,9]

$HC{\equiv}ReX_3$. The new C−H stretching modes at 3103.8 and 3097.3 cm^{-1} bracket the 3101.8 cm^{-1} value assigned to the $HC{\equiv}ReH_3$ complex,[6] and they are appropriate for the analogous $HC{\equiv}ReF_3$ and $HC{\equiv}ReCl_3$ methylidyne complexes. As shown in Figure 4, the 3097.3 cm^{-1} band shifts isotopically with the chloroform C−H stretching mode, but there are interesting differences. The ^{13}C shift of the product, 11.2 cm^{-1}, exceeds the 10.7 cm^{-1} shift for chloroform but is slightly less than the 12.2 cm^{-1} value calculated for the $HC{\equiv}ReCl_3$ complex. This means that carbon is vibrating more in the product mode than in the chloroform mode, which requires another heavier atom such as found in the $HC{\equiv}ReCl_3$ complex. In addition, the effect of fluorine substitution is to decrease the C−H stretching mode from 3053.4 cm^{-1} for $CHCl_3$ to 3043.5 cm^{-1} for CHF_3, but the product absorption blue-shifts with fluorine substitution. The H/D ratio for the product, 1.3296, is smaller than for the precursor, 1.3415, as expected from the above carbon isotopic difference. The observed and calculated frequencies are compared in Table 4. The Re−Cl stretching modes are below our 420 cm^{-1} spectral limit. However, two important modes are observed at 663.5 and 618.9 cm^{-1} for the $^{13}CHCl_3$ reaction, at 669 (shoulder) and 623.9 cm^{-1} for $^{12}CHCl_3$, and at 534.4 and 494.8 cm^{-1} for $CDCl_3$. These are in general agreement with the two (a″ and a′) H−C−Re bending modes calculated for the $HC{\equiv}ReCl_3$ complex using B3LYP (Table 4) but in better agreement with those calculated by using PW91 (Table S1). Notice that these bands are in the region

Table 4. Observed and Calculated Fundamental Frequencies of HC≡ReF_3 and HC≡$ReCl_3$ Complexes in the Ground $^2A'$ Electronic States with C_s Structures[a]

approximate description	HC≡ReF_3			HC≡$ReCl_3$			$H^{13}C$≡$ReCl_3$			DC≡$ReCl_3$		
	obs	calcd	int	obs	calcd	int	obs	calcd	int	obs	calcd	int
C−H stretch, a′	3103.8	3261.5	50	3097.3	3264.5	53	3086.1	3252.3	52	2329.4	2429.7	33
C≡Re stretch, a′		1098.2	9		1086.7	4		1050.6	3		1035.7	3
HCRe bend, a″	688.8	730.7	69	699	728.2	75	663.5	722.2	74	534.4	568.9	42
HCRe bend, a′	602.8	662.7	64	623.9	660.1	65	618.9	654.5	66	494.8	521.0	38
ReX_2 stretch, a′	657.1	657.8	174		387.4	69		387.4	70		386.8	65
Re−X stretch, a′	652.0	623.1	44		374.9	16		374.9	16		374.2	18
ReX_2 stretch, a″	614.1	611.9	96		370.4	47		370.4	47		370.3	48

[a] Frequencies and intensities are in cm^{-1} and km/mol, respectively. Five lower real frequencies are not listed. Observed natural isotopic frequencies in an argon matrix. Frequencies and intensities were calculated with B3LYP/6-311++G(3df,3pd), and the SDD pseudopotential and basis set are used for Re. The symmetry notations are based on the C_s structure

Table 5. Observed and Calculated Fundamental Frequencies of HC≡ReF_2Cl and HC≡$ReFCl_2$ Complexes in the Ground $^2A'$ Electronic States with C_s Structures[a]

approximate description	HC≡ReF_2Cl			$H^{13}C$≡ReF_2Cl			HC≡$ReFCl_2$			DC≡$ReFCl_2$		
	obs	calcd	int	obs	calcd	int	obs	calcd	int	obs	calcd	int
C−H stretch, a′	3101.6	3464.1	53	3090.6	3251.9	51	3099.5	3264.3	52	2331.1	2429.7	34
C≡Re stretch, a′		1094.2	6		1057.8	6	1090.2	682.1	6		1039.0	5
HCRe bend, a″	688.5	716.4	59	685.5	711.1	59	737.8	597.7	79	538.7	575.1	43
HCRe bend, a′	masked	664.7	12	masked	660.5	12	615.2	638.6	30	476.7	497.0	28
Re−F stretch, a′	644.5, 638.6	653.2	179	643.6, 638.2	651.3	179	638.6	647.6	164	634.8	630.6	130
Re−F stretch, a″	620.7, 615.8	614.2	94	620.3, 615.6	614.1	94						
Re−Cl stretch, a″		392.1	39		391.9	39	388.8		25		388.7	26
Re−Cl stretch, a′							371.7		49		371.6	50

[a] Frequencies and intensities are in cm^{-1} and km/mol, respectively. Five lower real frequencies are not listed. Observed natural isotopic frequencies in an argon matrix. Frequencies and intensities were calculated with B3LYP/6-311++G(3df,3pd), and the SDD pseudopotential and basis set are used for Re. The symmetry notations are based on the C_s structure.

Table 6. Optimized Energies and Geometry Parameters of YC≡ReX_3 (X, Y = H, F, Cl) Molecules[a]

molecule	state	ΔE	C−Y	C≡Re	Re−X_1	Re−X_2	∠HCRe	∠CReX_1	∠CReX_2
				C_{3v}					
$HCReH_3$	^2E	0	1.0861	1.725	1.678	1.678	180.0	97.7	97.7
$HCReF_3$	^2E	0	1.0856	1.729	1.909	1.909	180.0	107.6	107.6
$HCReCl_3$	^2E	0	1.0864	1.731	2.267	2.267	180.0	106.5	106.5
$FCReF_3$	^2E	0	1.2834	1.742	1.915	1.915	180.0	107.6	107.6
$ClCReCl_3$	^2E	0	1.6410	1.750	2.268	2.268	180.0	106.0	106.0
				C_s					
$HCReH_3$	$^2A'$	−6.96	1.0865	1.721	1.731	1.666	179.8	107.2	95.1
$HCReF_3$	$^2A'$	−11.61	1.0863	1.724	1.884	1.907	171.9	106.6	105.4
$HCReF_2Cl$	$^2A'$	−4.43	1.0864	1.726	2.246	1.909	173.7	106.1	106.3
$HCReFCl_2$	$^2A'$	−13.90	1.0866	1.728	1.894	2.274	173.9	109.9	103.9
$HCReCl_3$	$^2A'$	−4.89	1.0868	1.729	2.257	2.274	175.4	108.8	104.5
$FCReF_3$	$^2A'$	−6.96	1.2831	1.737	1.886	1.910	171.0	104.9	105.9
$ClCReCl_3$	$^2A'$	−11.61	1.6406	1.748	2.258	2.275	174.8	107.7	104.1

[a] All the energies (in kcal/mol) are calculated by using ZORA PW91/TZ2P. The bond lengths are in Å and bond angles in deg. X_1 and X_2 represent the one short and two long X ligands on Re. The ^2E states are calculated with average of configurations.

of acetylenic H−C−C−H bending modes[29] and that the observation of two such bands requires lower than three-fold symmetry and confirms experimentally that the HC≡$ReCl_3$ complex is distorted from a C_{3v} type of structure. The H/D ratios for the two bands, 1.249 and 1.252, are near the calculated value (1.267), but are considerably below the value for chloroform (1.339 for solid argon bands).

The two H−C−Re bending modes observed for the HC≡ReF_3 complex, 688.8 and 602.8 cm^{-1}, are in better agreement with the PW91 approximation. The 657.1 cm^{-1} band is appropriate for the strongest ReF_2 stretching mode predicted by our calculation for HC≡ReF_3 at 657.8 cm^{-1} and observed at 662.9 cm^{-1} for the analogous FC≡ReF_3 complex. The weaker 652.0 and 614.1 cm^{-1} bands follow for the other ReF_2 mode and the ReF mode calculated in this region using both density functionals. The extra weak, stable 628.8 cm^{-1} band is probably due to a binary ReF_x species which cannot be identified here.

Experiments with the mixed haloform precursors gave intermediate C−H stretching modes at 3101.6 and 3099.5 cm^{-1} for the corresponding HC≡ReF_2Cl and HC≡$ReFCl_2$ complexes, respectively. The ^{13}C shift for the former, 11.0 cm^{-1}, is almost the same as the corresponding 11.2 cm^{-1} shift for HC≡$ReCl_3$, and the C−D mode for DC≡$ReFCl_2$

(29) Herzberg, G. *Infrared and Raman Spectra*; D. Van Nostrand: Princeton, NJ, 1945.

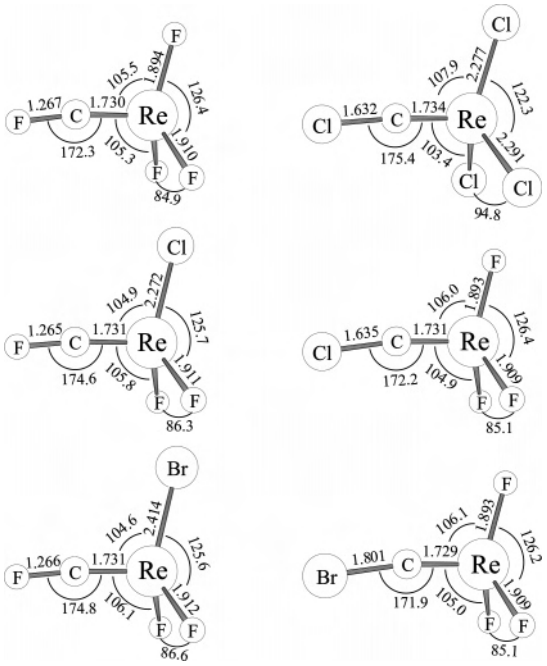

Figure 5. Structures of XC≡ReX$_3$ optimized at the levels of B3LYP/6-311++G(3df,3pd)/SDD. The bond lengths and angles are in Å and deg.

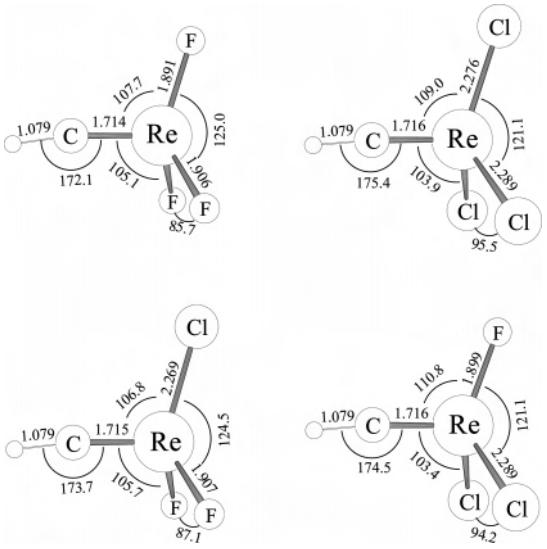

Figure 6. Structures of HC≡ReX$_3$ optimized at the levels of B3LYP/6-311++G(3df,3pd)/SDD. Similar PW91/TZ2P parameters are given in Table 7. The bond lengths and angles are in Å and deg.

at 2331.1 cm^{-1} bears the same relationship to the DC≡ReCl$_3$ mode at 2329.4 cm^{-1} as do the analogous C−H modes. The strongest two bands with the CHF$_2$Cl reagent at 644.5 and 638.6 cm^{-1} and weaker ones at 620.7 and 615.8 cm^{-1} appear to be due to split absorptions of matrix site for the symmetric and antisymmetric Re−F stretching modes calculated at 653.2 and 614.2 cm^{-1}, respectively, for the HC≡ReF$_2$Cl complex. The a″ component of the H−C−Re bending mode now appears at 688.6 cm^{-1} and shifts to 685.5 cm^{-1} with ^{13}C, and the weaker a′ component is probably masked by the strong precursor absorptions near 590 cm^{-1}. The single strong band at 638.6 cm^{-1} for the CHFCl$_2$ reaction shifts to 634.8 cm^{-1} with CDFCl$_2$, and this is appropriate for the Re−F stretching mode in the HC≡ReFCl$_2$ complex, which is mixed with the H(D)−C−Re bending mode. The pure

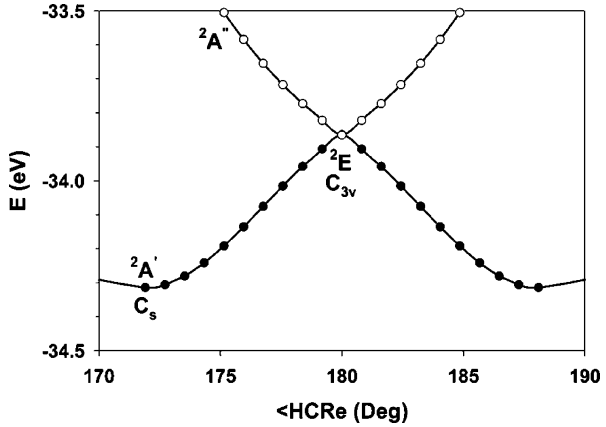

Figure 7. Linear synchronous transit energy curves of the two components of the ^{2}E state of the HC≡ReF$_3$ complex. The energies are calculated using scalar relativistic ZORA and the PW91 approach.

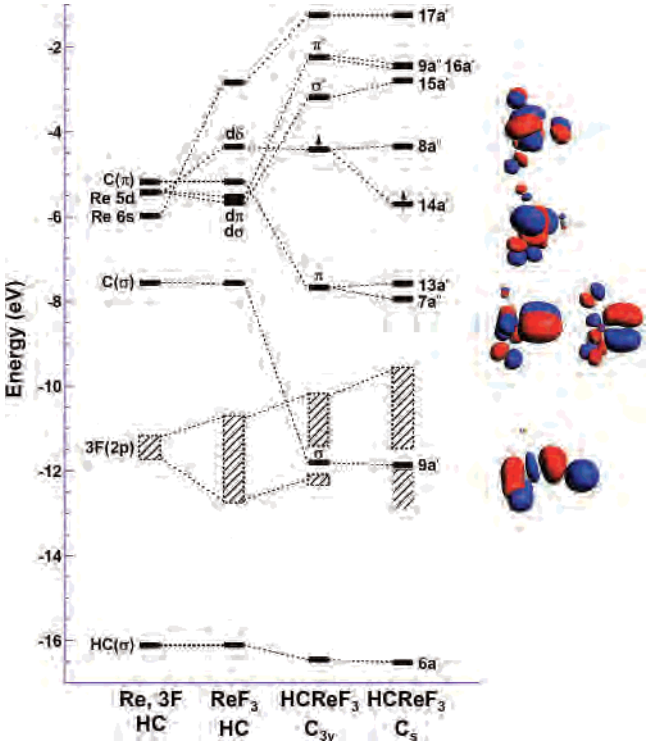

Figure 8. Energy levels of the HC≡ReF$_3$ complex in C_{3v} and C_s symmetry and orbital interactions between the fragment molecular orbitals. Only major orbitals are labeled and the arrow indicates the singly occupied molecular orbitals (SOMOs). The orbital energies are calculated using the scalar relativistic ZORA and PW91 approaches. The inset shows the isosurfaces of the four MOs involved in the C≡Re bond and the Jahn−Teller distortion (9a′, 7a″, 13a′, 14a′, and 8a″ orbitals from bottom to top).

PW91 density functional models this mode mixing better than the hybrid functional. The H−C−Re bending modes appear at 682.1 and 597.7 cm^{-1} and shift to 538.7 and 476.7 cm^{-1} on deuterium substitution (H/D ratios 1.266 and 1.254), which are diagnostic for the deformation mode in this complex. Our research shows that when using DFT to model vibrational modes for such complicated molecules, it is helpful to employ both hybrid and pure density functionals to accurately predict the vibrational properties.

The reaction with haloforms proceeds in the same manner as the tetrahalide precursors, viz, first through insertion and then α-halogen transfers to form the most stable methylidyne

Table 7. Calculated Diabatic Bond Energies (BE), Natural Charges (q), Natural Wiberg Bond Orders (BO), and s-Orbital Character of Carbon Hybridization for Selected $YC{\equiv}ReX_3$ Molecules[a]

	BE	BO	q_C	q_{Re}	s% (α)	s% (β)	s% (av)
$HCReH_3$	184.5	2.59	−0.23	0.55	46.73	46.08	46.41
$HCReF_3$	182.4	2.30	0.28	1.63	49.02	49.26	49.14
$HCReF_2Cl$	179.4	2.48	−0.22	1.40	48.78	48.54	48.66
$HCReFCl_2$	181.8	2.44	−0.19	1.09	48.31	48.31	48.31
$HCReCl_3$	178.3	2.38	−0.15	0.77	48.08	47.39	47.74
$FCReF_3$	206.0	2.30	0.28	1.63	34.01	34.60	34.31
$ClCReCl_3$	186.4	2.16	−0.11	0.77	39.68	39.37	39.53

[a] The zero-point-energy-corrected bond energies (in kcal/mol) are calculated using a scalar relativistic ZORA and PW91 approach. The natural bond orbital analysis was performed with B3LYP and the Gaussian 03 program.

product as summarized by reaction 3. The first sextet insertion product is more stable than the initial reagents by 59 kcal/mol, the quartet methylidene complex in the second step is more stable by 102 kcal/mol, and the final doublet ground state methylidyne by 132 kcal/mol at the B3LYP level of theory. The doublet-state methylidene intermediate complex is higher in energy than the quartet by 12 kcal/mol, and the quartet state $CH{=}ReCl_3$ complex is 48 kcal/mol higher than the doublet-state global minimum energy species. The α-hydrogen transfer $CCl_2{=}ReHCl$ methylidene is 36 kcal/mol higher in energy than the corresponding α-chlorine transfer $CHCl{=}ReCl_2$ complex, which shows why α-halogen transfer is favored in these reactions. Note the great stability of the carbyne complex, and reaction 3 is almost as exothermic as reaction 2.

$$Re + CHCl_3 \rightarrow [CHCl_2{-}ReCl]^* \rightarrow [CHCl{=}ReCl_2]^* \rightarrow HC{\equiv}ReCl_3 \quad (3)$$

Structure and Bonding in Rhenium Methylidyne Complexes. These rhenium methylidyne complexes are particularly interesting because of the unique C≡Re triple bonding and the distorted structures, which are tuned by the halogen substituents bonded to the metal center. The relative energies and geometry parameters of several selected $YC{\equiv}ReX_3$ (X = F, Cl; Y = H, F, Cl) complexes calculated by using the scalar relativistic ZORA and PW91 approach are listed in Table 6, which shows the Jahn−Teller distortion energies and the substituent effects on the geometric parameters of these complexes. For instance, the C−H and C≡Re distances and the ∠HCRe angles change regularly when F is substituted by Cl, which is consistent with our experiments (see below). The natural occupation numbers and the compositions of the natural localized molecular orbitals (NLMO) of these complexes are listed in Table 8 to provide intuitive understanding of the C≡Re triple bonds in these complexes.

Inasmuch as the relativistic effects are significant for the third-row transition metals, the electronic structures of these complexes are further complicated by the potential interaction of Jahn−Teller distortion and spin−orbit coupling. It is not obvious *a priori* which effect will dominate the doublet ground state of these unique rhenium methylidyne complexes. To understand the ground state and the structure of these complexes, we take the $HC{\equiv}ReF_3$ complex as an example to analyze the orbital interactions and the energy profile. Figure 7 shows the calculated scalar-relativistic energy curves using the LST approach and PW91 functional.

As mentioned earlier, the triple-bonded $HC{\equiv}ReF_3$ complex is the thermodynamically favored product for reaction of Re and CHF_3. One might expect that it has a linear ∠H−C−Re angle and a symmetric C_{3v} structure. Our calculations show that these $XC{\equiv}ReX_3$ complexes all adopt distorted structures rather than the C_{3v} structure. From the LST energy curves, it becomes clear that the spatially degenerate ^2E ground state of the C_{3v} structure will not be stable with respect to a vibrational mode of A′ symmetry, mainly a H−C−Re bending vibration. The first-order Jahn−Teller effect will distort the molecule along this mode to give rise to the C_s structure with shorter C≡Re bond length and nonlinear ∠H−C−Re angle.[30] In addition, the Re−F bond coplanar with the H−C−Re unit is shorter than the other two Re−F bonds by about 0.03 Å, a trend general with all of the halogen complexes studied (Table 6). The other component ($^2A''$) of the ^2E state will be stable at the C_{3v} symmetry, as indicated by the energy upsurge along the path of the Jahn−Teller distortion. Therefore, the ^2E state has one imaginary frequency and one real frequency calculated as 691i and 587 cm^{-1}, respectively, through the LST scan. The Jahn−Teller distortion along the A′ mode leads to a considerable energy stabilization, estimated to be some 0.45 eV (10 kcal/mol) from the LST energy curve.

Since spin−orbit coupling will split the singly occupied e-type molecular orbital into spinors $a_{3/2} + a_{3/2}^*$ and $e_{1/2}$, the Jahn−Teller effect would be quenched if the spin−orbit splitting is large enough. Our calculations using the spin−orbit ZORA approach show that, while the spin−orbit effect is indeed significant for Re 5d orbitals, it is not large enough to quench the substantial Jahn−Teller effect in these complexes. In fact, the Jahn−Teller splitting of the SOMO of the C_{3v} structure of $HC{\equiv}ReF_3$ is around 1.36 eV, whereas the first-order spin−orbit splitting of the SOMO is 0.32 eV at the level of PW91. Therefore, the ground states of these molecules are dictated by the Jahn−Teller effects, which is consistent with the experimental observation of three Re−F stretching modes for the $FC{\equiv}ReF_3$ complex and of two (a′ and a″) H−C−Re bending modes for the $HC{\equiv}ReF_3$ and $HC{\equiv}ReCl_3$ complexes.

The electronic structure of these rhenium methylidyne complexes can be understood through a fragment molecular orbital analysis. Figure 8 illustrates the orbital energy levels and orbital interactions of various molecular fragments of the $HC{\equiv}ReF_3$ complex, where only major molecular orbitals are labeled. The arrow indicates the singly occupied molecular orbitals (SOMOs). The inset showing the isosurfaces of the five MOs involved in the C≡Re bond and the Jahn−Teller distortion (9a′, 7a″, 13a′, 14a′, and 8a″ orbitals from bottom to top). All these energy levels were calculated using scalar relativistic ZORA and PW91 functional with the geometries of the fragments fixed at the optimized $HC{\equiv}ReF_3$ structure. The Re 6s and 5d orbitals are close in energy

(30) Herzberg, G. *Electronic Spectra of Polyatomic Molecules*; D. Van Nostrand: Princeton, NJ, 1966.

Table 8. NBO Occupation Numbers and the NLMO Compositions of YC≡ReX$_3$ Molecules from NBO Analysis[a]

	occ (α)	NLMO	occ (β)	NLMO
HC≡ReH$_3$	0.96	60% C($sp^{1.09}$) + 40% Re($sp^{0.18}d^{3.83}$)	0.98	57% C($sp^{1.97}$) + 43% Re($sp^{0.01}d^{5.32}$)
	0.99	38% C(p^1) + 62% Re(d^1)	0.99	44% C(p^1) + 56% Re(d^1)
	0.87	56% C($s^{0.05}p^1$) + 44% Re($s^{0.14}p^{0.24}d$)	0.95	53% C($sp^{3.97}$) + 47% Re($s^{0.12}d^1$)
HC≡ReF$_3$	0.97	67% C($sp^{0.56}$) + 33% Re($sd^{1.25}$)	0.98	68% C($sp^{0.53}$) + 32% Re($sd^{1.69}$)
	0.99	34% C(p^1) + 66% Re(d^1)	0.99	38% C(p^1) + 62% Re(d^1)
	0.83	53% C($s^{0.09}p^1$) + 47% Re($s^{0.05}p^{0.29}d$)	0.96	44% C(p^1) + 56% Re(d^1)
HC≡ReF$_2$Cl	0.97	62% C($sp^{0.97}$) + 38% Re($sd^{1.81}$)	0.98	62% C($sp^{0.95}$) + 38% Re($sd^{2.13}$)
	0.99	36% C(p^1) + 64% Re(d^1)	0.99	42% C(p^1) + 58% Re(d^1)
	0.82	50% C(p^1) + 50% Re($s^{0.04}p^{0.38}d$)	0.95	45% C(p^1) + 55% Re($s^{0.02}d^1$)
HC≡ReFCl$_2$	0.97	59% C($sp^{1.06}$) + 41% Re($sd^{2.38}$)	0.98	61% C($sp^{0.95}$) + 39% Re($sd^{2.62}$)
	0.99	34% C(p^1) + 66% Re(d^1)	0.97	40% C(p^1) + 60% Re(d^1)
	0.97	44% C($s^{0.03}p^1$) + 56% Re(d)	0.97	44% C(p^1) + 56% Re($s^{0.01}d^1$)
HC≡ReCl$_3$	0.98	59% C($sp^{0.96}$) + 41% Re($sd^{2.65}$)	0.98	61% C($sp^{0.91}$) + 39% Re($sd^{2.47}$)
	0.99	34% C(p^1) + 66% Re(d^1)	0.99	39% C(p^1) + 61% Re(d^1)
	0.97	38% C(p^1) + 62% Re($s^{0.02}$d)	0.96	41% C(p^1) + 59% Re(d^1)
FC≡ReF$_3$	0.97	67% C($sp^{0.56}$) + 33% Re($sd^{1.25}$)	0.98	68% C($sp^{0.53}$) + 32% Re($sd^{1.69}$)
	0.99	34% C(p^1) + 66% Re(d^1)	0.99	38% C(p^1) + 62% Re(d^1)
	0.83	53% C($s^{0.03}p^1$) + 47% Re($s^{0.05}p^{0.29}d$)	0.96	44% C(p) + 56% Re(d^1)
ClC≡ReCl$_3$	0.98	62% C($sp^{0.67}$) + 38% Re($sd^{2.56}$)	0.98	64% C($sp^{0.64}$) + 36% Re($sd^{2.38}$)
	0.99	35% C(p^1) + 65% Re(d^1)	0.99	40% C(p^1) + 60% Re(d^1)
	0.97	39% C(p^1) + 61% Re($s^{0.02}$d)	0.96	42% C(p) + 58% Re(d^1)

[a] All the NBO analyses were performed with Gaussian 03 using B3LYP with SDD ECP for Re and 6-311++G(2d,p) basis sets for nonmetal elements. The NLMO occupation numbers are slightly less than 1 for some π-NLMOs, indicating electron delocalization.

in the isolated atom, but the 6s orbital is destabilized significantly when three Re electrons were transferred to the F ligands upon formation of ReF_3 fragment. When Re is coordinated by three F ligands, the Re 5d orbitals are split as dσ < dπ ≪ dδ, where we denote the z^2, (xz, yz), and (xy, $x^2 - y^2$) orbitals as dσ, dπ, and dδ for convenience. The group orbitals (marked as shaded blocks) of the three F ligands stay together and broaden when F ligands are bonded to Re and when ReF_3 fragment is further bonded to HC fragment. The σ(C−H) bond of the HC fragment is slightly stabilized upon coordination to ReF_3 and marginally stabilized after Jahn−Teller distortion. The most significant bonding is for the C 2pσ and 2pπ orbitals, which are substantially stabilized by orbital interaction with the Re 5dσ and 5dπ orbitals when HC is coordinated to the ReF_3 fragment to form the C−Re σ and π bonds (labeled as σ and π in Figure 8), respectively. Consequently, the antibonding counterparts (labeled as σ* and π* in Figure 8) of the C≡Re triple bonds are destabilized to lie energetically above the weakly antibonding Re 5dδ orbitals. As a result, the 5dδ orbitals become the SOMO (showing with one unpaired electron in Figure 8), thus being subject to Jahn−Teller distortion.

Indeed, when the C_{3v} structure is relaxed via the Jahn−Teller effect, the Re 5d orbitals split into 14a′ + 8a″ orbitals in the C_s symmetry, where the 14a′ is markedly stabilized due to orbital mixing or hybridization of Re 6s and 5d orbitals. Detailed orbital analysis reveals that the SOMO is mainly composed of the $5d_{x^2-y^2}$ orbital (61%) in the original C_{3v} structure and after Jahn−Teller distortion significant mixing with Re 6s (10%) has been introduced into the SOMO, which facilitates better orbital overlap with the F ligand that is coplanar with the Re−C−H unit, as is shown by the isosurface of the 14a′ orbital. This 6s−5d hybridization explains why there is one short in-plane Re−F bond and two long out-of-plane Re−F bonds in the C_s structure. Interestingly, the simple HC≡ReH$_3$ complex was also shown to exhibit three Re−H stretching modes experimentally.[6] However, there is a minor difference in that for the hydride complex two Re−H bonds are calculated to be *shorter* by 4.1% than the longer unique Re−H bond, but for the halide complexes, two Re−X bonds are *longer* by 0.9 and 0.6% than the shorter unique Re−X bond for X = F and Cl, respectively. This subtle difference between the hydride complexes and the halide complexes is simply due to the orbital hybridization and the consequent structural difference in the pyramidal angle. In the HC≡ReH$_3$ complex, there is only 4% Re 6s mixing in the SOMO and therefore much less Re 6s−5d hybridization, as shown by the natural hybrid orbitals ($sp^{0.18}d^{3.83}$ vs $sd^{1.25}$) listed in Table 8, which leads to a much smaller pyramidal angle (∠H−Re−C) than the ∠X−Re−C (X = F, Cl) angles, as shown in Table 6. Because the two H atoms are nearly perpendicular to the H−C−Re axis, they can overlap with the Re 5dδ orbital in the SOMO to form two short and one long Re−H bonds, which is different from the aforementioned halide complexes that have much larger pyramidal angles.

Table 7 lists the calculated diabatic bond energies (BE), natural charges, natural Wiberg bond orders, and the s-orbital character of carbon hybridization for selected YC≡ReX$_3$ complexes of C_s symmetry. The BEs are corrected for zero-point energies from the calculated harmonic vibrational frequencies. All the Re atoms possess highly positive natural charge, particularly in the fluoro complexes, which is consistent with the ionic nature of the Re−halogen bonds. The NLMO calculations have clearly confirmed that there are C≡Re triple bonds in these rhenium methylidyne complexes: two Re−C (d−p)π bonds and one (sd^x−sp^y) σ bond with significant s-orbital character in the C and Re hybridization. The bond orders lie between 2.2 and 2.6 and decrease when H ligands are substituted by halogen on C or Re. The calculated diabatic bond energies for the C≡Re triple bonds are estimated to be between 180 and 210 kcal/mol.

It is noteworthy that the C−H stretching frequency (Figure 4) clearly varies with the number of F and Cl substituents on the metal center, which correlates well with the calculated bond distances and the natural hybrid orbitals (Tables 6 and 8). The diagnostic carbon−hydrogen stretching region is often congested which prevents the observation of important weak absorptions. The simple methylidyne product without interfering ligand chromophores allows observation of the elusive C−H stretching band of the H−C≡M subunit. The hydrogen stretching frequency increases with the amount of s-orbital character in the C−H bond from NBO analysis (Table 7),[31] and a C−H stretching frequency above 3000 cm^{-1} suggests increased s character, owing to orbital mixing or orbital hybridization.

Conclusions

In this work we report a series of simple, unique rhenium methlidyne complexes with halogen ligands attached to carbon and rhenium. These complexes were formed through reactions of laser-ablated rhenium atoms with various floro-, chloro-, and bromo-fluoromethanes. Matrix-isolation infrared spectra and quasi-relativistic density functional methods have been used to identify the new complexes formed in the experiments. Theoretical calculations using both hybrid and pure density functionals have provided strong support to the experimental assignment of the species and their spectra. Extensive bonding analyses are performed using natural bond orbitals and fragment molecular orbitals. These $XC{\equiv}ReX_3$ and $HC{\equiv}ReX_3$ complexes are shown to have significant Jahn−Teller distortion, which enhances the orbital interactions among carbon, rhenium, and the ligands. We have shown that the spin−orbit coupling effects are significant for rhenium complexes but are not large enough to quench the large Jahn−Teller effect. Therefore, the electronic structures and vibrational spectroscopic properties of the ground states of the third-row early transition-metal complexes can be interpreted using scalar-relativistic calculations. Spin−orbit effects can be treated as a perturbation for these ground-state properties. The discovery of these new rhenium methylidyne complexes is expected to promote further experimental and theoretical research on organometallic complexes with carbon−metal triple bonds.

Acknowledgment. We gratefully acknowledge financial support from NSF Grant No. CHE 03-52487 to L.A. This work is also supported by NKBRSF (2006CB932305) and NNSFC (20525104) of China. The calculations were performed by using a HP Itanium2 cluster at the National Laboratory for Information Science and Technology at Tsinghua University.

Supporting Information Available: DFT results. This material is available free of charge via the Internet at http://pubs.acs.org.

IC701014U

(31) Pavia, D. L.; Lampman, G. M.; George, S. K. *Introduction to Spectroscopy*, 3rd Ed.; Brooks Cole: New York, 2000.